NUCLEIC ACID THERAPEUTICS
Volume 24, Number 6, 2014

DOI: 10.1089/nat.2014.0493

Tumor Cell–Targeted Delivery of Nanoconjugated Oligonucleotides in Composite Spheroids

Kyle Carver, Xin Ming, and Rudy L. Juliano

Standard tissue culture has often been a poor model for predicting the efficacy of anti-cancer agents including oligonucleotides. In contrast to the simplicity of monolayer tissue cultures, a tumor mass includes tightly packed tumor cells, tortuous blood vessels, high levels of extracellular matrix, and stromal cells that support the tumor. These complexities pose a challenge for delivering therapeutic agents throughout the tumor, with many drugs limited to cells proximal to the vasculature. Multicellular tumor spheroids are superior to traditional monolayer cell culture for the assessment of cancer drug delivery, since they possess many of the characteristics of metastatic tumor foci. However, homogeneous spheroids comprised solely of tumor cells do not account for some of the key aspects of metastatic tumors, particularly the interaction with host cells such as fibroblasts. Further, homogeneous culture does not allow for the assessment of targeted delivery to tumor versus host cells. Here we have evaluated delivery of targeted and untargeted oligonucleotide nanoconjugates and of oligonucleotide polyplexes in both homogeneous and composite tumor spheroids. We find that inclusion of fibroblasts in the spheroids reduces delivery efficacy of the polyplexes. In contrast, targeted multivalent RGD–oligonucleotide nanoconjugates were able to effectively discriminate between melanoma cells and fibroblasts, thus providing tumor-selective uptake and pharmacological effects.

Introduction

Tumors include many types of host cells, most prominently fibroblasts. Activated fibroblasts are key modulators of metastasis through promoting invasion, migration, and growth of cancer cells. This is achieved through degradation of the extracellular matrix (ECM) and basement membrane of the primary tumor as well as by providing support at the distal site by the production of growth factors and other components [1–3]. However, not all of the fibroblasts within a tumor are harmful to the patient; carcinoma-associated fibroblasts are able to express both tumor promoting and tumor suppressing molecules [4,5]. Normal fibroblasts can suppress tumor growth and progression [1,4]. Therefore, it is usually desirable for therapeutic agents to be able to affect cancer cells without harming fibroblasts or other host cells.

Oligonucleotides can potentially provide effective and selective therapy of cancer [6,7]. However, the utility of these compounds for therapy has been limited due to the difficulty in delivering them to their sites of action within specific cells of the tumor [8–10]. Various nanoparticle formulations have been utilized for delivery of oligonucleotides [11,12]. Nanoparticles are advantageous due to the fact that they are large enough to escape renal clearance and can passively target tumors through the enhanced permeation and retention effect [13]. However, nanoparticles tend to accumulate proximal to the blood vessels, leaving distal portions of the tumor untreated [14,15]. The lack of diffusion is a result of the composition and geometry of the ECM along with tightly packed cells of the tumor, limiting the pore size of the extracellular space [16].

Tumor spheroids mimic the structure of metastatic lesions and are more relevant for assessing drug delivery than monolayer cultures [17,18]. We have shown previously that human serum albumin (HSA) nanoconjugates with multiple arginine-glycine-aspartic acid (RGD) peptides are able to effectively penetrate and distribute in a tumor spheroid model [19]. The peptide RGD serves as a ligand for the integrin receptor $\alpha_V\beta_3$ [20], which has increased expression in some cancers and is associated with progression of metastasis [21]. Furthermore, we have shown that these conjugates are superior to larger nanoparticles for delivering oligonucleotides to cells within a tumor spheroid [22]. However, these tumor spheroids were formed from melanoma cells alone and therefore could not be utilized for determining differential delivery to tumor versus host cells. In this study, we utilized a more complex tumor spheroid comprised of melanoma cells and human dermal fibroblasts. We assessed both the ability of

Division of Molecular Pharmaceutics, Eshelman School of Pharmacy, University of North Carolina, Chapel Hill, North Carolina.

our RGD conjugates to distribute throughout the complex spheroid and the specificity with which the nanoconjugates target cancer cells.

Methods

Cell culture

A375 human melanoma cells were stably transfected with a firefly luciferase (A375 Luc705) [23] expression cassette containing a mutated intron. The mutated intron can be removed by using a splice switching oligonucleotide, thus giving inducible expression of the reporter, as described previously [24]. An A375 cell line with a constitutive green fluorescent protein expression cassette was also used. Human dermal fibroblasts (HDF) at passage 18 were obtained from the Tissue Culture Facility at the University of North Carolina and used between passages 20 and 28. All cells were grown in high glucose Dulbecco's modified Eagle's medium (DMEM) media (Sigma) supplemented with 10% fetal bovine serum (FBS).

Generation of multicellular tumor spheroids

Multicellular tumor spheroids (MCTS) were generated using the hanging drop method described previously [22]. Briefly, cells were trypsinized and resuspended in 20% FBS high glucose DMEM at a concentration to achieve 3000 cells per 30 μL for single cell MCTS or 13000 A375 Luc705 and 3000 HDF cells per 30 μL for composite MCTS. In a 72-microwell plate (Nunc 438733, Thermo Fisher Scientific), 30 μL was added to each well; plates were then inverted and incubated at 37°C for 3–5 days on an orbital shaker. Once formed, MCTS, 10 spheroids per well, were transferred to a 48 well plate coated with 1.5% agarose for treatment.

Oligonucleotide formulation and cell treatment

The splice switching oligonucleotide 623 (SSO623) [5′-GTTATTCTTTAGAATGGTGC-3′], which can correct the mutated introns in Luc705 constructs and induce reporter gene expression [23], or its five base mismatch control [5′-GTAATTATTTATAATCGTCC-3], were used in all experiments. A 3′ carboxytetramethylrhodamine (TAMRA) labeled version of 623 was also used (SSO623-T). Complexes of a cationic polymer (jetPEI; Polyplus) with SSO623-T were prepared per the vendor's instructions. These polyplexes are approximately 300 nM in size [25]. Preparation of a morpholino (PMO) version of SSO623 conjugated to human serum albumin (HSA) (HSA-PMO) as well as an RGD-PMO conjugate (HSA-PMO-RGD) were performed as described previously [19]. These nanoconjugates also include an Alexa 488 fluorophore. The HSA-PMO and HSA-PMO-RGD conjugates are about 13 nm in diameter and thus are substantially smaller than most oligonucleotide nanocarriers [19]. In both spheroid models, uptake of polyethylenimine 623 (PEI-623), HSA-PMO, and HSA-PMO-RGD was performed in 10% FBS DMEM. All groups were treated for 16 hours. Spheroids were washed to remove any remaining nanoconjugate and incubated an additional 48 hours before being harvested for analysis.

Luciferase assay

Cells were washed with phosphate buffered saline before being digested with luciferase lysis buffer (New England Biolabs) at a dilution of 1:4 in double-distilled water. After centrifugation, 50 μL of luciferin substrate (Promega) was added to 20 μL of lysate and luciferase activity was measured in a plate reader (FLUOstar Omega; BMG Labtech) over a 5-second window. The sum of blank corrected data over seconds 2–5 of the window was used to quantitate induction. Induction was normalized to protein concentration measured with a bovine serum albumin assay (Thermo Scientific).

Flow cytometry

Spheroids were trypsinized and fixed in single cell suspension with 4% paraformaldehyde. In some cases cells were incubated with a fibroblast-selective cluster of differentiation 90 (CD90) antibody conjugated to APC (Life Technologies) before being resuspended in phosphate-buffered saline (PBS) for flow cytometry on an LSR II using a 488 nm laser with 510/20 bandpass filter (green fluorescent protein/Alexa 488), 561-nm laser with 610/20 bandpass (TAMRA), and 639-nm laser with 675/20 bandpass (Alexa 633/APC). After gating for live singlet cells, cells were gated for APC flourescence to differentiate melanoma cells from HDFs. Uptake was quantified by normalizing mean Alexa 488 (HSA-623 and HSA-623-RGD) or TAMRA (PEI-SSO623-T) fluorescence value with the control cell's autofluorescence.

Histology

MCTS were harvested and fixed in 4% paraformaldehyde before being embedded in 1.5% agarose molds to maintain orientation. These molds were then placed in 70% ethanol and stored prior to being embedded in paraffin and sectioned. Serial slides were processed with Masson's trichrome to demonstrate the density of cells as well as collagen content.

Immunofluorescence

MCTS were harvested and fixed in 4% paraformaldehyde before being cryoprotected in 30% sucrose in PBS. Spheroids were placed in a 1.5% agarose block in order to maintain orientation before being embedded in optimal cutting temperature (OCT) medium (Sakura) and sectioned. Slides with serial interrupted sections were stained with a CD90 antibody conjugated to allophycocyanin (APC) and exposed to 4′,6-diamidino-2-phenylindole (DAPI) prior to being mounted. Images were collected on a Leica DMIRB inverted microscope using a 10× objective and HQ2 color camera (Photometrics).

Results

Characterization of complex spheroids

We have shown previously that A375 melanoma cells will form tumor spheroids with densely packed cells but limited extracellular matrix [22]. In order to determine how the addition of fibroblasts affects the growth and morphology of the tumor spheroids, A375 spheroids were developed with and without human dermal fibroblasts (HDF). The complex spheroids developed much quicker, taking 2–3 days compared with 5–7 days for A375 cells alone, and required increased trypsinization to dissociate, 60 minutes compared to 5 minutes (data not shown). In support of these observations, Masson's trichrome stain shows that the complex spheroids are more uniform and circular, have more tightly packed

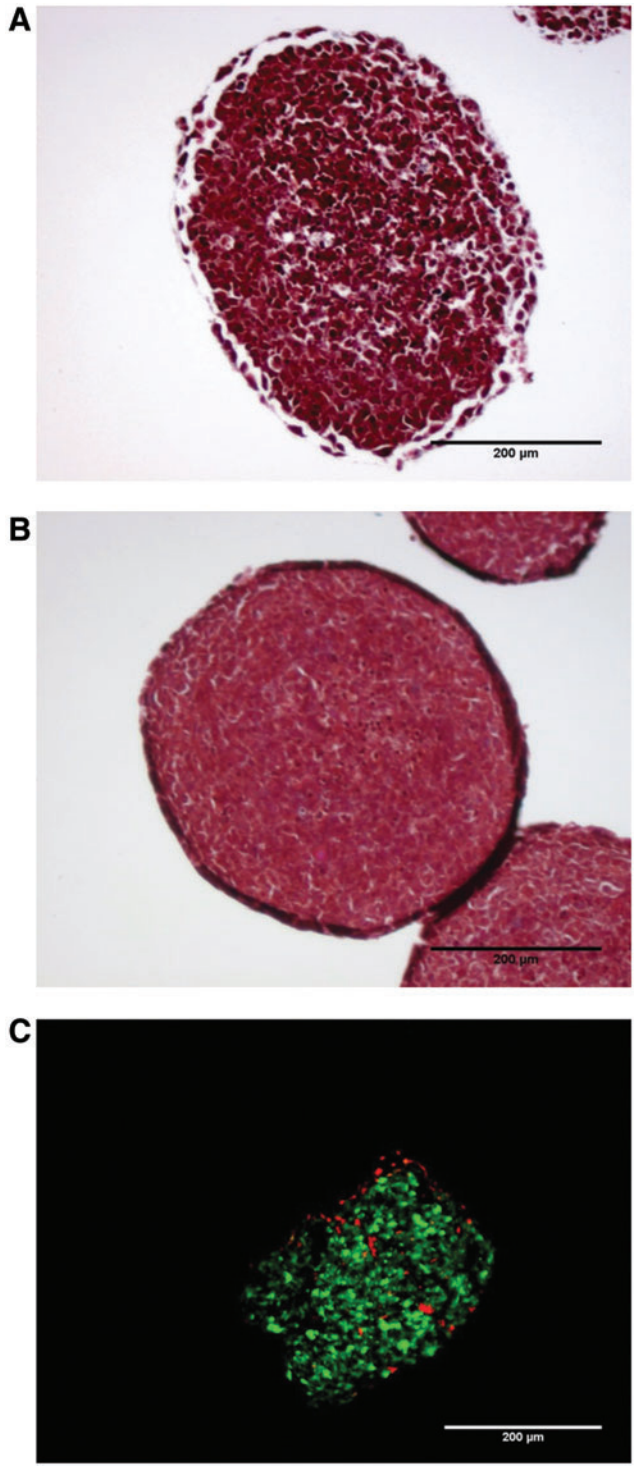

FIG. 1. Spheroid morphology. Spheroids grown from **(A)** A375 human melanoma cells transfected with a firefly luciferase (A375 Luc705) or **(B)** A375 Luc705 and human dermal fibroblast (HDF) cells were fixed prior to paraffin embedding. Sections of spheroids were stained using Masson's trichrome. The purple staining in the interstices between cells represents extracellular matrix. **(C)** A375 green fluorescent protein (GFP) + HDF spheroids were fixed and embedded in optimal cutting temperature (OCT) medium prior to sectioning. Sections were stained with cluster of differentiation 90-allophycocyanin antibody (CD90-APC) prior to imaging. Scale bar represents 200 μm. Color images available online at www.liebertpub.com/nat

cells, and have increased extracellular matrix (Fig. 1A, B). Expression of CD90 was measured to differentiate the melanoma cells from fibroblasts in the complex spheroids (Supplementary Figs S1, S2; Supplementary Data are

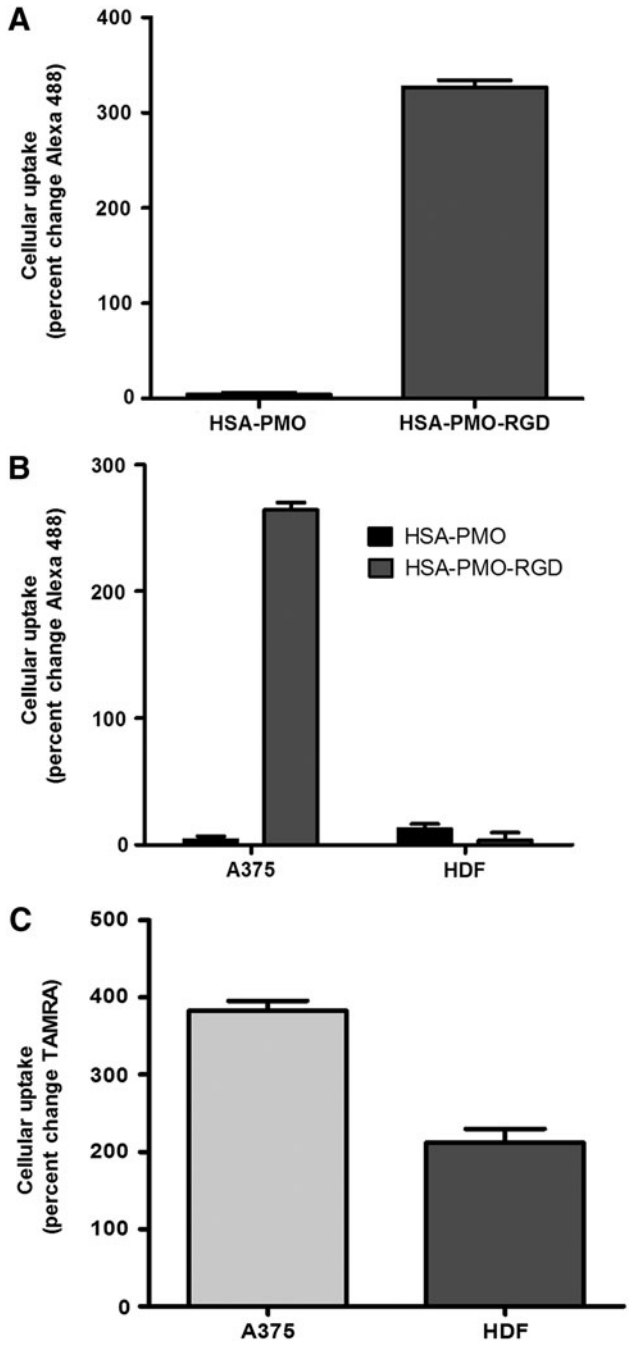

FIG. 2. Nanoparticle uptake in spheroids. **(A)** A375Luc705 and **(B)** A375Luc705 + HDF spheroids were incubated with either HSA-PMO or HSA-PMO-RGD (human serum albumin-morpholino-[arg-gly-asp]) at 100 nM for 16 hours. **(C)** A375Luc705 + HDF spheroids were incubated with SSO623-polyethyleneimine (PEI) at 100 nM for 16 hours. After the incubation period spheroids were dispersed with trypsin, fixed, and stained with CD90-APC prior to fluorescent measurements by flow cytometry. Uptake is measured as percent change compared with untreated control spheroids and represented as mean ± standard error of the mean (SEM). $n = 4–7$.

available online at www.liebertpub.com/nat). The distribution of HDF within the spheroid is heterogeneous (Fig. 1 C).

Targeted uptake of oligonucleotide conjugates

One of the primary challenges for cancer therapeutics is attaining the ability to direct drugs selectively to the cells of interest without damaging the surrounding normal tissue. In A375 spheroids, the RGD-linked targeted nanoconjugates increased delivery over 80-fold compared to the unliganded conjugates (Fig. 2 A). Interestingly, there was little loss of enhanced targeted delivery in the complex spheroids, with a 60-fold increase over non-RGD control nanoconjugates (Fig. 2 B). Furthermore, when uptake in HDFs was assessed there was no difference between the two conjugates, suggesting that the RGD-conjugate was differentially targeting the melanoma cells. Complex spheroids were also treated with a SSO623-TAMRA cationic polymer (jetPEI) complex to assess nonspecific uptake of a typical oligonucleotide polyplex (Fig. 2C). While there was a high degree of uptake of SSO623 into the A375 cells, there was also substantial uptake into the fibroblasts of the spheroids suggesting that the non-targeted polyplex delivery would affect both tumor and normal cells. Additionally, in previous studies we have shown that similar

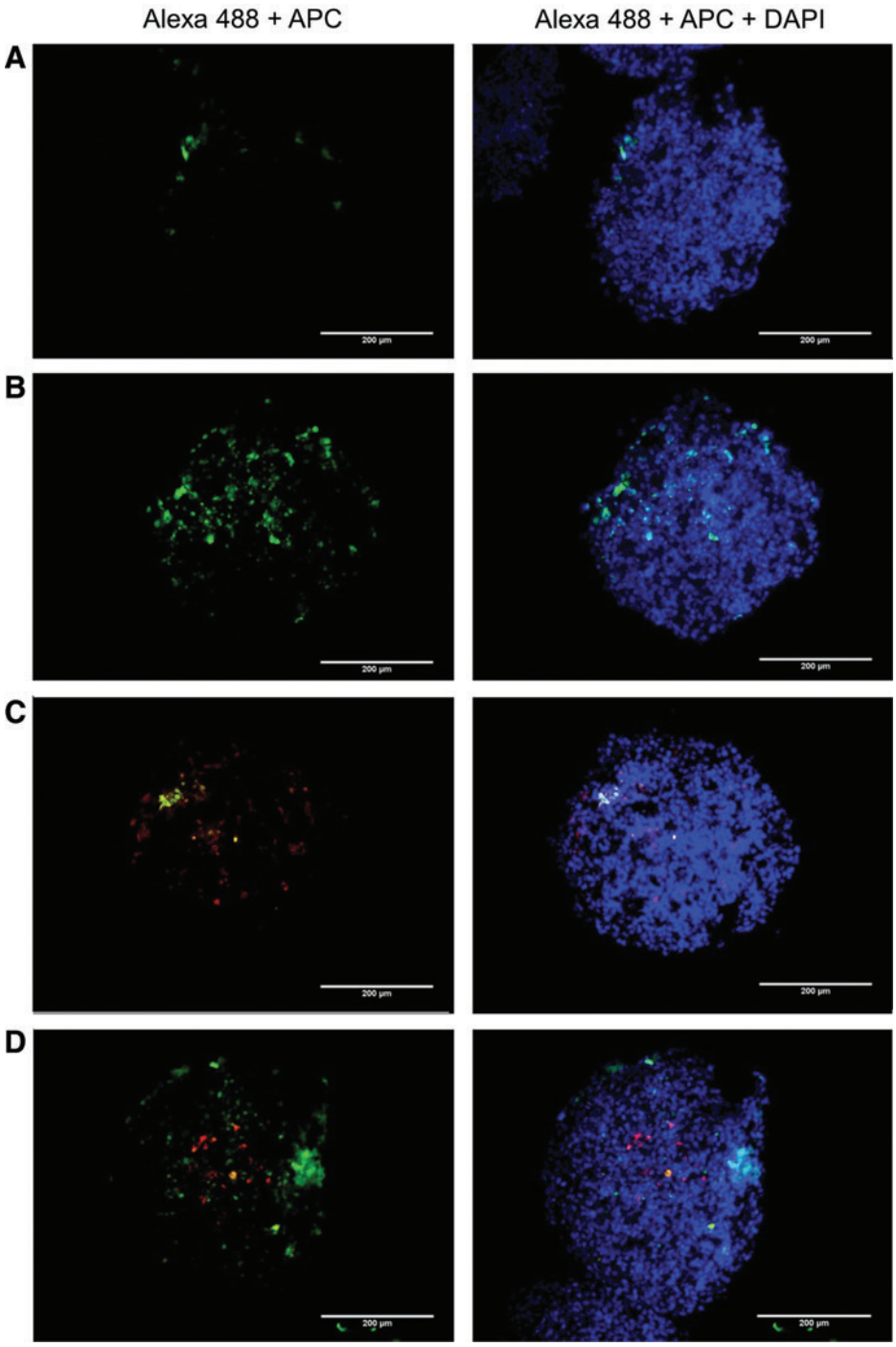

FIG. 3. Nanoparticle uptake in spheroid sections. Spheroids grown from A375Luc705 were treated with either **(A)** HSA-PMO or **(B)** HSA-PMO-RGD and spheroids grown from A375Luc705 + HDF cells were treated with either **(C)** HSA-PMO or **(D)** HSA-PMO-RGD for 16 hours. Spheroids were fixed and embedded in OCT prior to sectioning. Spheroid sections were stained with CD90-APC prior to imaging. *Blue*, DAPI, 4′,6-diamidino-2-phenylindole; *green*, Alexa 488; *red*, APC. Scale bar represents 200 µm. Color images available online at www.liebertpub.com/nat

PEI complexes primarily affect cells at or near the surface of the spheroid [22]. Taken together these data demonstrate that the HSA-SSO623-RGD conjugates are able to both increase cellular uptake and specifically target melanoma cells within the complex spheroid.

Flow cytometry is unable to tell us where in the spheroid the conjugates are distributing. To assess the distribution of the nanoconjugates within the two spheroid models, we imaged frozen sections of treated spheroids stained with a CD90-APC antibody. As expected, there was no positive staining of CD90 in the A375-only spheroids (Fig. 3A, B). In spheroids treated with HSA-PMO, there was minor uptake in the periphery of the spheroid with no penetration (Fig. 3 A), while the conjugates with RGD were able to effectively penetrate and distribute throughout the spheroid (Fig. 3B). Similar to the results shown in Fig. 2B, uptake of HSA-PMO in the complex spheroids was primarily in the fibroblasts that were located on the periphery of the spheroid (Fig. 3C). Treatment of the complex spheroids with HSA-PMO-RGD results in distribution similar to that seen in the A375 only spheroid with the majority of conjugate being taken up by the melanoma cells, demonstrated by little colocalization between Alexa 488 and APC (Fig. 3 D).

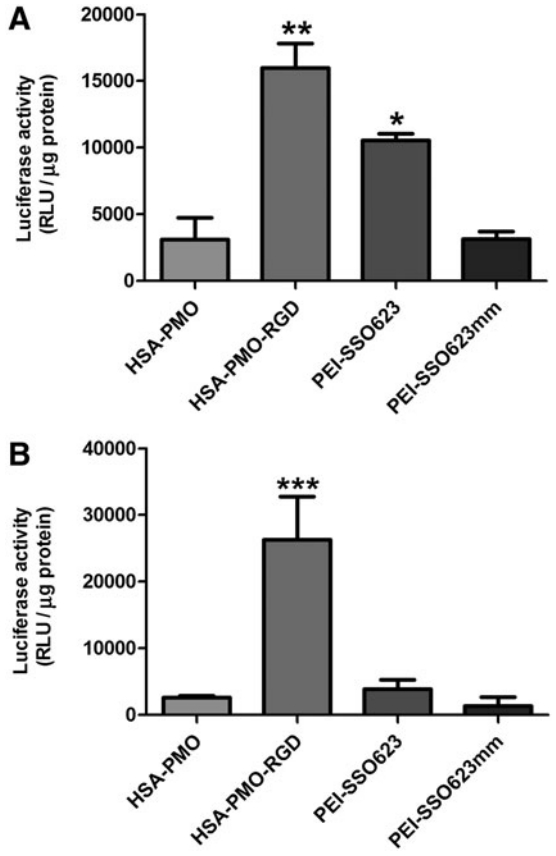

FIG. 4. Induction of luciferase in spheroids. **(A)** A375Luc705 and **(B)** A375Luc705 + HDF spheroids were incubated with either HSA-PMO, HSA-PMO-RGD, PEI-SSO623, or PEI-SSO623mm at 100 nM for 16 hours and then incubated for a further 48 hours. Spheroids were dispersed and subsequent cell suspension lysed in a luciferase buffer. Luciferase activity was measured on a FLUOstar Omage plate reader and quantified as relative luminescence units per µg protein after subtracting control, untreated spheroid, values and depicted as mean ± SEM. $n = 3$–10. $^{*}p < 0.05$ compared with HSA-PMO. $^{**}p < 0.01$ compared with HSA-PMO and SSO623mm-PEI. $^{***}p < 0.001$ compared with all other groups.

Splice-switching efficacy

We examined the ability of the nanoconjugates and the polyplexes to elicit a biological effect. Complex and simple spheroids were formed from A375-Luc705 melanoma cells with and without HDFs, respectively, and treated with HSA-PMO, HSA-PMO-RGD, SSO623-PEI, or SSO623mm-PEI. Induction of luciferase by SSO623mm-PEI was used as a negative control. In both spheroid types, the levels of luciferase activity induced by the HSA-PMO conjugate was similar to that of the mismatch control (Fig. 4A, B). Importantly, the HSA-PMO-RGD conjugate was able to significantly increase luciferase activity compared with control in both the simple and complex spheroids. Treatment of simple spheroids with SSO623-PEI resulted in a similar increase in luciferase activity to that of the RGD conjugate. However, interestingly, in the complex spheroid the induction capacity of the PEI complex was significantly attenuated down to control levels. The reduction in luciferase activity in the complex spheroids is most likely due to a combination of more tightly packed cells with increased ECM deposition and preventing effective penetration, along with nonspecific uptake into fibroblasts. These data suggest that while the addition of fibroblasts reduces biological effect of larger polyplex complexes, it does not affect that of the smaller targeted oligonucleotide nanoconjugates.

Discussion

There is a clear need to develop improved therapeutics that can effectively target the lesions in advanced cancer. However, the use of monolayer cell cultures for drug screening, with their lack of similarity to the tumor microenvironment, has led to inefficient translation from *in vitro* studies to *in vivo* therapies [17]. The three-dimensional tumor spheroid model has been suggested to represent an *in vitro* system similar to that of micrometastases [26]. In fact, it has been suggested that certain cancers utilize endogenous spheroid formation to survive transit through the peritoneal cavity to sites of metastasis [18]. In addition, recent studies have shown that metastases require the support of stromal cells for continuous growth and propagation [1–3]. These observations suggest that a co-culture tumor spheroid model featuring cancer cells with fibroblasts would improve the physiological relevance as well as providing a means for studying targeted drug delivery.

To further increase the verisimilitude to tumors *in vivo*, one might consider including vascular endothelial cells, lymphocytes and macrophages into the spheroid since these all play important roles in tumor biology and are potential therapeutic targets [27]. However, practical constraints may come into play as more cell types are added. We have shown that inclusion of fibroblasts in A375 tumor spheroids increases the tightness and ECM deposition of the spheroid (Fig. 1). The use of a fluorescently conjugated CD90 antibody effectively discriminates between the fibroblasts and cancer cells of the spheroid and thus helps to define oligonucleotide delivery.

Due to the support stromal cells provide for metastasis, it has been suggested that fibroblasts could pose a potential

therapeutic target [28,29]. However, it has also been recently suggested that not all of the fibroblasts within a tumor are harmful to the patient; carcinoma associated fibroblasts are able to express both tumor promoting and tumor suppressing molecules simultaneously [4,5]. In addition, normal fibroblasts—those that have not been activated by the cancer cells—can suppress tumor growth and progression [1]; primary fibroblasts from a tumor are able to reduce the growth of co-cultured cancer cells *in vitro* [4]. Therefore, direct targeting of cancer cells should prove to be a more advantageous method of therapy than ubiquitous cell death within the tumor by leaving the hosts natural defenses intact.

Utilizing the complex tumor spheroid model we demonstrate that an oligonucleotide nanocarrier comprised of albumin conjugated with multiple RGD ligands can specifically target melanoma cells over human dermal fibroblasts (Fig. 2). Furthermore, these conjugates can distribute and deliver oligonucleotides throughout the spheroid while larger complexes and non-targeted conjugates are confined to the periphery of the spheroid (Fig. 3). The lack of observable uptake of the non-RGD HSA conjugates deep within the spheroid could be due to poor penetration of the conjugate; alternatively, the conjugate may possibly penetrate into the spheroid but fail to be taken up into cells, resulting in the conjugate being washed away during processing steps.

Oligonucleotides are potentially useful therapeutic agents for cancer. However, the result of non-targeted delivery to host cells is a reduction in efficacy and possible off-target actions. We demonstrate such an effect with delivery of SSO623 to the complex spheroid using a cationic polyplex. Uptake of the polyplex into fibroblasts is accompanied by a significant attenuation of the luciferase induction effect in tumor cells (Fig. 4). The RGD nanoconjugates, on the other hand, were targeted specifically to the A375 melanoma cells and showed no reduction in luciferase induction between simple and complex spheroids. In fact, there appeared to be a greater level of induction in the complex spheroids, which could possibly be a result of growth promoting effects of fibroblasts.

Our studies suggest that RGD is an effective targeting ligand for melanoma cells and, to the extent that complex tumor spheroids represent *in vivo* micrometastasis, the inclusion of RGD into nanoconjugates is a superior method for oligonucleotide delivery compared to non-targeted conjugates or large cationic polyplexes. This general approach may have utility for other types of oligonucleotides such as siRNA and could employ other types of targeting ligands such as aptamers. However, ultimately the capacity for targeted delivery by RGD nanoconjugates will require validation *in vivo*. This would include demonstration of selective uptake by tumor cells as opposed to host cells as well as evidence of tumor growth inhibition.

Acknowledgment

This study was funded by National Institutes of Health R01 CA151964 to RLJ.

Author Disclosure Statement

No competing financial interests exist.

References

1. Kalluri R and M Zeisberg. (2006). Fibroblasts in cancer. Nat Rev Cancer 6:392–401.
2. Strell C, H Rundqvist and A Ostman. (2012). Fibroblasts–a key host cell type in tumor initiation, progression, and metastasis. Ups J Med Sci 117:187–195.
3. Xing F, J Saidou and K Watabe. (2010). Cancer associated fibroblasts (CAFs) in tumor microenvironment. Front Biosci (Landmark Ed) 15:166–179.
4. Augsten M. (2014). Cancer-associated fibroblasts as another polarized cell type of the tumor microenvironment. Front Oncol 4:62.
5. Madar S, I Goldstein and V Rotter (2013). 'Cancer associated fibroblasts'–more than meets the eye. Trends Mol Med 19:447–453.
6. Bennett CF and EE Swayze. (2010). RNA targeting therapeutics: molecular mechanisms of antisense oligonucleotides as a therapeutic platform. Annu Rev Pharmacol Toxicol 50: 259–293.
7. Watts JK and DR Corey. (2012). Silencing disease genes in the laboratory and the clinic. J Pathol 226:365–379.
8. Juliano R, J Bauman, H Kang and X Ming. (2009). Biological barriers to therapy with antisense and siRNA oligonucleotides. Mol Pharm 6:686–695.
9. Juliano RL, K Carver, C Cao and X Ming. (2013). Receptors, endocytosis, and trafficking: the biological basis of targeted delivery of antisense and siRNA oligonucleotides. J Drug Target 21:27–43.
10. Kaneda Y. (2010). Update on non-viral delivery methods for cancer therapy: possibilities of a drug delivery system with anticancer activities beyond delivery as a new therapeutic tool. Expert Opin Drug Deliv 7:1079–1093.
11. Dassie JP and PH Giangrande. (2013). Current progress on aptamer-targeted oligonucleotide therapeutics. Ther Deliv 4:1527–1546.
12. Presente A and SF Dowdy. (2013). PTD/CPP peptide-mediated delivery of siRNAs. Curr Pharm Des 19:2943–2947.
13. Maeda H, H Nakamura and J Fang. (2013). The EPR effect for macromolecular drug delivery to solid tumors: Improvement of tumor uptake, lowering of systemic toxicity, and distinct tumor imaging in vivo. Adv Drug Deliv Rev 65:71–79.
14. Kostarelos K, D Emfietzoglou, A Papakostas, WH Yang, A Ballangrud and G Sgouros. (2004). Binding and interstitial penetration of liposomes within avascular tumor spheroids. Int J Cancer 112:713–721.
15. Li L, J Sun and Z He. (2013). Deep penetration of nanoparticulate drug delivery systems into tumors: challenges and solutions. Curr Med Chem 20:2881–2891.
16. Ishida T and H Kiwada. (2013). Alteration of tumor microenvironment for improved delivery and intratumor distribution of nanocarriers. Biol Pharm Bull 36:692–697.
17. E LB, YC Hsu and JA Lee. (2014). Consideration of the cellular microenvironment: physiologically relevant co-culture systems in drug discovery. Adv Drug Deliv Rev 69–70:190–204.
18. Sodek KL, KJ Murphy, TJ Brown and MJ Ringuette. (2012). Cell-cell and cell-matrix dynamics in intraperitoneal cancer metastasis. Cancer Metastasis Rev 31:397–414.
19. Ming X, K Carver and L Wu. (2013). Albumin-based nanoconjugates for targeted delivery of therapeutic oligonucleotides. Biomaterials 34:7939–7949.
20. Marelli UK, F Rechenmacher, TR Sobahi, C Mas-Moruno and H Kessler. (2013). Tumor targeting via integrin ligands. Front Oncol 3:222.
21. Desgrosellier JS and DA Cheresh. (2010). Integrins in cancer: biological implications and therapeutic opportunities. Nat Rev Cancer 10:9–22.

22. Carver K, X Ming and RL Juliano. (2014). Multicellular tumor spheroids as a model for assessing delivery of oligonucleotides in three dimensions. Mol Ther Nucleic Acids 3:e153.
23. Alam MR, V Dixit, H Kang, ZB Li, X Chen, J Trejo, M Fisher and RL Juliano. (2008). Intracellular delivery of an anionic antisense oligonucleotide via receptor-mediated endocytosis. Nucleic Acids Res 36:2764–2776.
24. Ming X, MR Alam, M Fisher, Y Yan, X Chen and RL Juliano. (2010). Intracellular delivery of an antisense oligonucleotide via endocytosis of a G protein-coupled receptor. Nucleic Acids Res 38:6567–6576.
25. Ming X, K Sato and RL Juliano. (2011). Unconventional internalization mechanisms underlying functional delivery of antisense oligonucleotides via cationic lipoplexes and polyplexes. J Control Release 153:83–92.
26. Friedrich J, R Ebner and LA Kunz-Schughart. (2007). Experimental anti-tumor therapy in 3-D: spheroids–old hat or new challenge? Int J Radiat Biol 83:849–871.
27. Fang H and YA Declerck. (2013). Targeting the tumor microenvironment: from understanding pathways to effective clinical trials. Cancer Res 73:4965–4977.
28. Pietras K and A Ostman. (2010). Hallmarks of cancer: interactions with the tumor stroma. Exp Cell Res 316:1324–1331.
29. Togo S, UM Polanska, Y Horimoto and A Orimo. (2013). Carcinoma-associated fibroblasts are a promising therapeutic target. Cancers (Basel) 5:149–169.

Address correspondence to:
Rudolph L. Juliano, PhD
Eshelman School of Pharmacy
University of North Carolina
1072 Genetic Medicine Building
Chapel Hill, NC 27599

E-mail: arjay@med.unc.edu

Received for publication May 21, 2014; accepted after revision August 4, 2014.